

Manuscript Number: WR38976R1

Title: Combining stable isotopes with contamination indicators: a method for improved investigation of nitrate sources and dynamics in aquifers with mixed nitrogen inputs

Article Type: Research Paper

Keywords: Nitrate; Groundwater; Stable isotope; Contamination indicator; Diffuse source pollution; Point source pollution

Corresponding Author: Dr. Eddy P Minet, PhD

Corresponding Author's Institution: Dublin City Council

First Author: Eddy P Minet, PhD

Order of Authors: Eddy P Minet, PhD; Robbie Goodhue, PhD; Wolfram Meier-Augenstein, PhD; Robert M Kalin, PhD; Owen Fenton, PhD; Karl G Richards, PhD; Catherine E Coxon, PhD

Abstract: Excessive nitrate (NO₃⁻) concentration in groundwater raises health and environmental issues that must be addressed by all European Union (EU) member states under the Nitrates Directive and the Water Framework Directive. The identification of NO₃⁻ sources is critical to efficiently control or reverse NO₃⁻ contamination that affects many aquifers. In that respect, the use of stable isotope ratios ¹⁵N/¹⁴N and ¹⁸O/¹⁶O in NO₃⁻ (expressed as δ¹⁵N-NO₃⁻ and δ¹⁸O-NO₃⁻, respectively) has long shown its value. However, limitations exist in complex environments where multiple nitrogen (N) sources coexist. This two-year study explores a method for improved NO₃⁻ source investigation in a shallow unconfined aquifer with mixed N inputs and a long established NO₃⁻ problem. In this tillage-dominated area of free-draining soil and subsoil, suspected NO₃⁻ sources were diffuse applications of artificial fertiliser and organic point sources (septic tanks and farmyards). Bearing in mind that artificial diffuse sources were ubiquitous, groundwater samples were first classified according to a combination of two indicators relevant of point source contamination: presence/absence of organic point sources (i.e. septic tank and/or farmyard) near sampling wells and exceedance/non-exceedance of a contamination threshold value for sodium (Na⁺) in groundwater. This classification identified three contamination groups: agricultural diffuse source but no point source (D+P⁻), agricultural diffuse and point source (D+P⁺) and agricultural diffuse but point source occurrence ambiguous (D+P[±]). Thereafter δ¹⁵N-NO₃⁻ and δ¹⁸O-NO₃⁻ data were superimposed on the classification. As δ¹⁵N-NO₃⁻ was plotted against δ¹⁸O-NO₃⁻, comparisons were made between the different contamination groups. Overall, both δ variables were significantly and positively correlated (p < 0.0001, r_s = 0.599, slope of 0.5), which was indicative of denitrification. An inspection of the contamination groups revealed that denitrification did not occur in the absence of point source contamination (group D+P⁻). In fact, strong significant denitrification lines occurred only in the D+P⁺ and D+P[±] groups (p < 0.0001, r_s > 0.6, 0.53 ≤ slope ≤ 0.76), i.e. where point source

contamination was characterised or suspected. These lines originated from the 2-6‰ range for $\delta^{15}\text{N-NO}_3^-$, which suggests that i) NO_3^- contamination was dominated by an agricultural diffuse N source (most likely the large organic matter pool that has incorporated ^{15}N -depleted nitrogen from artificial fertiliser in agricultural soils and whose nitrification is stimulated by ploughing and fertilisation) rather than point sources and ii) denitrification was possibly favoured by high dissolved organic content (DOC) from point sources. Combining contamination indicators and a large stable isotope dataset collected over a large study area could therefore improve our understanding of the NO_3^- contamination processes in groundwater for better land use management. We hypothesise that in future research, additional contamination indicators (e.g. pharmaceutical molecules) could also be combined to disentangle NO_3^- contamination from animal and human wastes.

HIGHLIGHTS

- Groundwater samples were collected from an aquifer with mixed N inputs
- N source apportionment was first based on indicators of point source contamination
- $\delta^{15}\text{N}$ and $\delta^{18}\text{O}$ in NO_3^- were then superimposed to N source apportionment
- The dominant source of groundwater NO_3^- was characterised (agricultural diffuse)
- Conditions for denitrification were identified (point source contamination)

1 **Combining stable isotopes with contamination indicators: a method for improved investigation**
2 **of nitrate sources and dynamics in aquifers with mixed nitrogen inputs**

3

4

5 E.P. Minet^{1,5*}, R. Goodhue¹, W. Meier-Augenstein^{2,3}, R.M. Kalin^{2,4}, O. Fenton⁵, K.G. Richards⁵, C.E.
6 Coxon^{1*}

7

8 ¹ Geology Department, School of Natural Sciences, Trinity College Dublin, Dublin 2, Ireland

9 ² Environmental Engineering Research Centre, David Keir Building, Queen's University Belfast,
10 Stranmillis Road, Belfast BT9 5AG, Northern Ireland

11 ³ New address: School of Pharmacy and Life Sciences, Sir Ian Wood Building, Robert Gordon
12 University, Garthdee Road, Aberdeen AB10 7GJ, Scotland

13 ⁴ New address: David Livingstone Centre for Sustainability, Level 6, Graham Hills Building, 50
14 Richmond Street, Strathclyde University, Glasgow G1 1XN, Scotland

15 ⁵ Teagasc Environment Research Centre, Johnstown Castle, Co. Wexford, Ireland

16

17 * Authors to whom correspondence should be addressed:

18 Eddy P. Minet

19 Email: eddy.minet@gmail.com

20

21 Catherine E. Coxon

22 Geology Department

23 School of Natural Sciences

24 Trinity College Dublin

25 Dublin 2, Ireland

26 Email: cecoxon@tcd.ie

27

28

29 **ABSTRACT**

30 Excessive nitrate (NO_3^-) concentration in groundwater raises health and environmental issues that
31 must be addressed by all European Union (EU) member states under the Nitrates Directive and the
32 Water Framework Directive. The identification of NO_3^- sources is critical to efficiently control or
33 reverse NO_3^- contamination that affects many aquifers. In that respect, the use of stable isotope ratios
34 $^{15}\text{N}/^{14}\text{N}$ and $^{18}\text{O}/^{16}\text{O}$ in NO_3^- (expressed as $\delta^{15}\text{N}-\text{NO}_3^-$ and $\delta^{18}\text{O}-\text{NO}_3^-$, respectively) has long shown its
35 value. However, limitations exist in complex environments where multiple nitrogen (N) sources
36 coexist. This two-year study explores a method for improved NO_3^- source investigation in a shallow
37 unconfined aquifer with mixed N inputs and a long established NO_3^- problem. In this tillage-
38 dominated area of free-draining soil and subsoil, suspected NO_3^- sources were diffuse applications of
39 artificial fertiliser and organic point sources (septic tanks and farmyards). Bearing in mind that
40 artificial diffuse sources were ubiquitous, groundwater samples were first classified according to a
41 combination of two indicators relevant of point source contamination: presence/absence of organic
42 point sources (i.e. septic tank and/or farmyard) near sampling wells and exceedance/non-exceedance
43 of a contamination threshold value for sodium (Na^+) in groundwater. This classification identified
44 three contamination groups: agricultural diffuse source but no point source (D+P-), agricultural
45 diffuse and point source (D+P+) and agricultural diffuse but point source occurrence ambiguous
46 (D+P±). Thereafter $\delta^{15}\text{N}-\text{NO}_3^-$ and $\delta^{18}\text{O}-\text{NO}_3^-$ data were superimposed on the classification. As $\delta^{15}\text{N}-$
47 NO_3^- was plotted against $\delta^{18}\text{O}-\text{NO}_3^-$, comparisons were made between the different contamination
48 groups. Overall, both δ variables were significantly and positively correlated ($p < 0.0001$, $r_s = 0.599$,
49 slope of 0.5), which was indicative of denitrification. An inspection of the contamination groups
50 revealed that denitrification did not occur in the absence of point source contamination (group D+P-).
51 In fact, strong significant denitrification lines occurred only in the D+P+ and D+P± groups ($p <$
52 0.0001 , $r_s > 0.6$, $0.53 \leq \text{slope} \leq 0.76$), i.e. where point source contamination was characterised or
53 suspected. These lines originated from the 2-6‰ range for $\delta^{15}\text{N}-\text{NO}_3^-$, which suggests that i) NO_3^-
54 contamination was dominated by an agricultural diffuse N source (most likely the large organic matter
55 pool that has incorporated ^{15}N -depleted nitrogen from artificial fertiliser in agricultural soils and
56 whose nitrification is stimulated by ploughing and fertilisation) rather than point sources and ii)

57 denitrification was possibly favoured by high dissolved organic content (DOC) from point sources.
58 Combining contamination indicators and a large stable isotope dataset collected over a large study
59 area could therefore improve our understanding of the NO_3^- contamination processes in groundwater
60 for better land use management. We hypothesise that in future research, additional contamination
61 indicators (e.g. pharmaceutical molecules) could also be combined to disentangle NO_3^- contamination
62 from animal and human wastes.

63

64

65 **KEY WORDS**

66 Nitrate; Groundwater; Stable isotope; Contamination indicator; Diffuse source pollution; Point source
67 pollution

68

69

70 **1 INTRODUCTION**

71 Elevated levels of nitrate (NO_3^-) in aquifers have long been a cause of concern (Stark and Richards,
72 2008). If ingested, contaminated groundwater is potentially harmful to human and animal health.
73 From an environmental perspective, discharge into surface-water bodies can contribute to eutrophic
74 conditions in lakes, streams, estuaries and the coastal zone. Groundwater NO_3^- also represents a
75 source of indirect nitrogen (N) losses which occur as a result of partial denitrification of NO_3^- into
76 nitrous oxide (N_2O), a powerful greenhouse gas. Eventually, such contamination issues may have
77 detrimental knock-on effects on the economy (Sutton et al., 2011). In response to the elevated NO_3^-
78 levels recorded in many water bodies, the European Union (EU) has implemented a number of
79 directives (e.g. Nitrates 91/676/EEC, Water Framework 2000/60/EC, Groundwater 2006/118/EC) that
80 establish a range of measures to reduce NO_3^- contribution from agricultural and non-agricultural
81 sources (Stark and Richards, 2008). Yet controlling groundwater contamination by NO_3^- is still a
82 challenging task, and many EU aquifers have remained heavily contaminated since the introduction of
83 the Nitrates Directive in 1991 (van Grinsven et al., 2012). Reasons for the mixed results are multiple
84 and include the lag-time between measures implementation and improved water quality, the lack of

85 follow through from local actors, but also the complexity of the N cycle and a poor understanding of
86 some *in-situ* mechanisms (Oenema et al., 2011). Additional tools are therefore required to identify the
87 causes of contamination and spatially target existing and future environmental measures. Ideally,
88 accurate NO_3^- source identification is a necessary first step if the contamination problem is to be
89 efficiently addressed. In complex systems however, where several types of NO_3^- sources coexist,
90 source identification and determination of relative contributions become complicated. Such
91 uncertainty is typically witnessed in intensive agricultural areas with high human population densities.
92 In an Irish tillage-dominated catchment historically associated with high NO_3^- occurrence for instance,
93 two studies had attributed the NO_3^- problem to either organic point N sources (stored farmyard wastes
94 and livestock housing, septic tanks) (Daly, 1981) or diffuse applications of artificial N fertilisers
95 (Coxon and Thorn, 1991).

96

97 Discriminating between NO_3^- sources such as artificial fertiliser and animal/human organic effluents
98 in rural areas has been central to water studies for decades. Among the methods used to track NO_3^- are
99 dual stable isotope analyses, which measure $^{15}\text{N}/^{14}\text{N}$ and $^{18}\text{O}/^{16}\text{O}$ ratios in dissolved NO_3^- (expressed
100 as $\delta^{15}\text{N}\text{-NO}_3^-$ and $\delta^{18}\text{O}\text{-NO}_3^-$, respectively). The interest in this technique came from the expectation
101 that some of the major N sources involved in the terrestrial N cycle generate NO_3^- with characteristic
102 and therefore recognizable δ values in groundwater (Kendall et al., 2007). However, NO_3^- is not a
103 conservative ion and once in soil, it is likely to undergo some biochemical reactions and isotopic
104 fractionation that can greatly affect the original δ characteristic values. Heterotrophic denitrification in
105 soil and subsoil is often the cause of a major kinetic isotope effect due to a ^{15}N enrichment factor $\epsilon_{\text{N}_2\text{-NO}_3}$
106 NO_3 (atmospheric dinitrogen N_2 is the reaction product and NO_3^- the substrate) that can vary between -
107 40‰ and -5‰ (Kendall et al., 2007). The consequence of this nitrate removal for the residual NO_3^-
108 pool is that $\delta^{15}\text{N}\text{-NO}_3^-$ and $\delta^{18}\text{O}\text{-NO}_3^-$ increase linearly over a wide range of values along a slope often
109 reported for groundwater between 0.5 and 0.8 (Granger and Wankel, 2016). This isotopic enrichment
110 in the heavier isotopes can result in NO_3^- from (or derived from) artificial fertiliser displaying $\delta^{15}\text{N}\text{-NO}_3^-$
111 NO_3^- in the range expected for NO_3^- derived from organic wastes (Kendall et al., 2007). The early
112 stage of nitrification in non N-limited systems (e.g. a fertilised field) on the other hand can cause the

113 first newly formed NO_3^- to be quite ^{15}N -depleted compared with the ammonia substrate (NH_3) due to a
114 ^{15}N enrichment factor $\epsilon_{\text{NO}_3\text{-NH}_3}$ recorded by some between -38‰ and -5‰ (Kendall et al., 2007). But
115 as the N pool is used up, the nitrification rate decreases and so does the isotopic fractionation so that
116 $\delta^{15}\text{N-NO}_3^-$ of newly formed nitrate increases toward the original $\delta^{15}\text{N-NH}_3$ of the substrate over time.
117 The consequence is that leached NO_3^- can display a wide range of $\delta^{15}\text{N-NO}_3^-$ values as nitrification
118 proceeds (Kendall et al., 2007). Finally, mineralisation-immobilisation turnover processes (MIT) (i.e.
119 the rapid remineralisation of NO_3^- assimilated by soil microflora) alter $\delta^{18}\text{O-NO}_3^-$ to within the range
120 expected from nitrification (Mengis et al., 2001) so that synthetic NO_3^- from artificial fertilisers loses
121 its original atmospheric oxygen atoms and therefore its characteristic $\delta^{18}\text{O-NO}_3^-$ signature. As a result,
122 large overlaps may occur between N source types early during the leaching process within the
123 unsaturated zone (Fogg et al., 1998; Minet et al., 2012), hence weakening NO_3^- source tracking in
124 underlying groundwater (Kendall et al., 2007; Xue et al., 2009). More complications can combine
125 within the aquifers under the action of mixing processes between NO_3^- sources, further NO_3^- removal
126 by denitrification (Kendall et al., 2007) and concurrent NO_3^- production during anammox under
127 anoxic conditions (Granger and Wankel, 2016).

128

129 To reduce the uncertainties over source identification and fate of NO_3^- , recent research has combined,
130 with a varying degree of success, $\delta^{15}\text{N-NO}_3^-$ and $\delta^{18}\text{O-NO}_3^-$ with a number of source apportionment
131 models (Davis et al., 2015; Kim et al., 2015; Xue et al., 2015), groundwater flow dynamics (Hosono
132 et al., 2013), isotopes from non-N species (Stoewer et al., 2015), $\delta^{15}\text{N}$ from nitrogenous species other
133 than NO_3^- (Wells et al., 2016), pharmaceutical markers (Fenech et al., 2012) and/or hydrochemical
134 parameters (Pastén-Zapata et al., 2014). The interest in hydrochemistry comes from the fact that
135 besides NO_3^- , many N sources also contain and contribute to the leaching of other ions, which may
136 impact groundwater quality and increase concentrations above natural background levels (NBL)
137 otherwise observed under uncontaminated conditions. Farm animal wastes and septic tank effluents
138 for instance are typically enriched in chloride (Cl^-), potassium (K^+) and sodium (Na^+) amongst many
139 other contaminants, which are all released by decomposing organic matter (Ranjbar and Jalali, 2012).
140 Septic tanks effluents may be further enriched in Na^+ due to human salty diet, the use of water

141 softeners and detergents. Na^+ concentration in farm slurry tanks and septic tank effluents have been
142 commonly measured up to 700 mg L^{-1} (Mulqueen et al., 1999; Sommer and Husted, 1995) and 100
143 mg L^{-1} (Richards et al., 2016) respectively. Consequently Na^+ , which is one of the most mobile of the
144 common cations with low affinity for soil exchange sites (Weil and Brady, 2017), has been used by
145 others as a chemical tracer to delineate plumes of contamination from human organic effluents
146 (Robertson et al., 1991). Yet elevated Na^+ concentration in groundwater used alone can only confirm
147 that contamination by organic wastes occurred. Unlike stable isotopes in NO_3^- , it will not inform on
148 the relative contribution of an organic point source to the NO_3^- issue.

149

150 This paper describes a methodology of NO_3^- source identification whereby $\delta^{15}\text{N-NO}_3^-$ and $\delta^{18}\text{O-NO}_3^-$
151 data were analysed after first classifying groundwater samples according to a combination of
152 contamination indicators. The first indicator was visual and arose from a N source risk assessment
153 survey, with the second indicator being Na^+ concentration in groundwater. This second indicator was
154 used because i) Na^+ is a major component of N-rich organic effluents discharged from septic tanks
155 and farmyards, ii) Na^+ is absent from all main artificial fertilisers applied in the study area, iii) the
156 diffuse application of organic animal wastes was not an important N source and iv) the Na^+ NBL
157 value was low (13 mg L^{-1} in Tedd et al. (2017)). The purpose of this preliminary classification was to
158 apportion groundwater contamination to existing N sources using conventional methods, whereas the
159 superimposition of $\delta^{15}\text{N-NO}_3^-$ and $\delta^{18}\text{O-NO}_3^-$ data on this classification was to specifically inform on
160 the contributions of these N sources to NO_3^- contamination and dynamics. Overall, the objective of
161 this study was to explore the applicability of this method for improved investigation of NO_3^- sources
162 and dynamics in the complex environment of the above-mentioned Irish catchment with multiple
163 contamination diffuse and point N sources.

164

165

166 **2 MATERIALS AND METHODS**

167 **2.1 Study area description**

168 **2.1.1 Geology and soil**

169 Groundwater sampling took place in the Barrow Valley (south-east Ireland) across three sites that
170 cover 40 km² (Fig.1). The bedrock consists of strata of Carboniferous limestone which underlie
171 Quaternary deposits consisting mainly of fluvio-glacial sand and gravel. Quaternary deposit thickness
172 is highly variable but can be up to 25 m, while the individual sand and gravel units, which are usually
173 very coarse, can be up to 10 m thick. Soils are generally well drained. Further details are available in
174 Section 2.1.1 of Materials and Methods SM.

175

176

177 **2.1.2 Hydrogeology**

178 There were three main types of aquifers (Fig.1): i) a largely unconfined and highly to extremely
179 vulnerable shallow Quaternary sand and gravel aquifer, which encompasses most sampling wells, ii) a
180 karstic aquifer and iii) a poorly productive bedrock aquifer. Groundwater flow at the regional scale is
181 towards the south and towards the River Barrow (Daly, 1981), although local groundwater pathways
182 can be unpredictable due to the flat topography. Annual rainfall during the sampling period ranged
183 between 606 and 917 mm, whereas annual effective rainfall (i.e. rainfall minus evapotranspiration
184 minus surface runoff), whose daily variations are reported in Fig.2, varied between 179 mm and 464
185 mm. Groundwater recharge, accounted for by effective rainfall, mostly occurred between October and
186 April of each year, when the soil moisture deficit (SMD) was nil (Fig.2). Air temperature followed a
187 seasonal pattern around its mean (9.6 °C) typical of a temperate maritime climate (Fig.2). A similar
188 pattern was observed with groundwater temperature around 11.5 °C (Fig.2). Further details are
189 available in Section 2.1.2 of Materials and Methods SM.

190

191

192 **2.1.3 Land use and management**

193 Soils were primarily dedicated to tillage (Fig.SM-1, adapted from EPA (2017)) for barley and wheat
194 production (64% of land use). Grassland (35% of land use) was used for pasture, silage and hay.
195 Fertilisation largely involved the diffuse application of synthetic non-N (e.g. potash KCl) and N
196 fertilisers, the most popular one by far being Calcium Ammonium Nitrate (CAN). N inputs at the time
197 of the study were routinely excessive for some crops (Teagasc Crop Advisor Officer, personal
198 communication). Due to the predominant tillage land use, the diffuse application of organic animal
199 wastes was not an important N source within the study area. The farm and farmyard density was about
200 1.7 km⁻². Despite few specialising in beef production, many housed some livestock and therefore had
201 some potentially leaking farmyards and manure storage systems. The density of population ranged
202 between 20 and 30 persons km⁻². Typically for a rural area, most dwellings were not connected to a
203 public sewerage system, but had their own septic tank instead. Further details are available in Section
204 2.1.3 of Materials and Methods SM.

205

206

207 **2.1.4 Sampling wells**

208 Groundwater samples were collected from 45 wells (Table SM-1). All but one well (B9) were
209 satisfactorily capped and not directly open to air. The type of aquifer intercepted was Quaternary
210 deposits only or Quaternary deposits and bedrock. Further details are available in Section 2.1.4 of
211 Materials and Methods SM.

212

213

214 **2.2 Data collection**

215 **2.2.1 Groundwater sampling**

216 233 groundwater samples were collected at low and high groundwater recharge times during six
217 sampling campaigns (Fig.2). Each well was generally visited five times or more. Samples were
218 collected directly from the closest tap, which was flamed and cleansed with ethanol, then turned on
219 for up to five minutes to flush the pipe and get water representative of the aquifer. Monitoring

220 boreholes were purged and sampled with a peristaltic pump. All samples were kept chilled in a cool
221 box during transport to the laboratory. Samples aimed for hydrochemistry analysis and NO_3^-
222 extraction (Section 2.2.2) were filtered on the day of collection with 0.45 μm nylon-membranes
223 before being stored overnight at 4 °C. Further details are available in Section 2.2.1 of Materials and
224 Methods SM.

225

226

227 **2.2.2 Groundwater quality and stable isotopes measurements**

228 Groundwater samples were analysed for thirteen physico-chemical and microbial parameters:
229 temperature, conductivity, alkalinity, pH, ion concentrations (NO_3^- , Cl^- , sulphate (SO_4^{2-}), Na^+ , K^+ ,
230 magnesium (Mg^{2+}), calcium (Ca^{2+})), coliforms (total TC and faecal FC). After NO_3^- concentrations
231 were measured, an aliquot of each groundwater sample containing 100 μmol of NO_3^- was portioned
232 off and extracted according to a simplified ion-exchange resin method best suited for freshwater
233 samples with high NO_3^- ($> 25 \text{ mg L}^{-1}$) and low dissolved organic carbon (DOC) levels (typically < 5
234 mg C L^{-1}) (Minet et al., 2011). $\delta^{15}\text{N-NO}_3^-$ and $\delta^{18}\text{O-NO}_3^-$ were determined by Continuous-Flow
235 Isotope Ratio Mass Spectrometry in duplicate for each AgNO_3 sample encapsulated in silver boats.
236 $\delta^{15}\text{N-NO}_3^-$ and $\delta^{18}\text{O-NO}_3^-$ values were expressed in permil (‰) relative to Air and VSMOW
237 respectively, using the standard definition of the δ value of the heavier isotope (h) of a given chemical
238 element (E), $\delta^h\text{E} = \{(\text{R}_{\text{sample}} - \text{R}_{\text{std}}) / \text{R}_{\text{std}}\}$, where R represents $^{15}\text{N}/^{14}\text{N}$ or $^{18}\text{O}/^{16}\text{O}$ ratios in samples
239 (R_{sample}) and standards (R_{std}) (Kendall et al., 2007). $\delta^{18}\text{O-H}_2\text{O}$ and $\delta^2\text{H-H}_2\text{O}$ were measured in
240 groundwater samples collected between September 2002 and September 2003 (118/233 samples).
241 Further details are available in Section 2.2.2 of Materials and Methods SM.

242

243

244 **2.2.3 N source risk assessment**

245 A N source risk assessment survey was carried out within a 300 m radius around each sampling well.
246 Two main types of N sources reported in Table SM-2 were identified: i) organic point sources, which
247 include septic tanks from unsewered houses and farmyards with potential for N-enriched plumes of

248 contamination and ii) agricultural diffuse sources, which include artificial N fertiliser applications to
249 intensively managed land (tillage and grassland) and soil organic matter (i.e. crop residues, plants,
250 micro- and macro-organisms). Importantly, diffuse sources were ubiquitous as each sampling well
251 was surrounded by more than 75% of intensively managed agricultural land (Table SM-2). % tillage
252 was also estimated because it has long been suspected to be related to diffuse N source contamination
253 in this region (Coxon and Thorn, 1991). Further details are available in Section 2.2.3 of Materials and
254 Methods SM.

255

256

257 **2.3 Data analysis**

258 **2.3.1 *Sample classification and N source apportionment***

259 Groundwater samples were classified according to a two-step methodology (Fig.3). The purpose was
260 to apportion contamination to N source types (Section 3.3.1) using conventional methods before
261 analysing $\delta^{15}\text{N-NO}_3^-$ and $\delta^{18}\text{O-NO}_3^-$ (Section 3.3.2). In Step 1, groundwater samples were classified
262 based on the presence/absence of organic point sources within a 300 m radius of sampling wells using
263 N source risk assessment data (Table SM-2). To increase the power of the classification, it was
264 decided to add the second indicator. In Step 2, groundwater was classified based on the
265 exceedance/non-exceedance of a Na^+ contamination threshold (CT), Na^+ being a major component of
266 N-rich organic effluents discharged from septic tanks and farmyards. Any exceedance of the CT value
267 was deemed indicative of point source contamination because Na^+ is not a major constituent of the
268 main artificial fertilisers applied in the study area (unlike other indicators like Cl^- and K^+) and animal
269 waste was not an important diffuse N source (Section 2.1.3). This CT value was not strictly speaking
270 a NBL but it gave a picture of the Na^+ concentration in the less contaminated groundwater. It was
271 calculated as the 75th percentile of Na^+ concentration from twenty-nine low NO_3^- samples ($< 25 \text{ mg L}^-$
272 ¹) from the study area (Section 3.3.1) in order to exclude outliers from groundwater highly
273 contaminated by a point source but severely denitrified. The main limitation of Step 2 came from the
274 fact that Na^+ is not as mobile in soils as NO_3^- , but it is nonetheless one of the most mobile of the

275 common cations whose adsorption should be further reduced as the sorption sites within plumes of
276 contamination become saturated.

277

278 Where both steps of the classification agreed over the impact (or the lack of impact) of point sources,
279 the origin of contamination was deemed beyond reasonable doubt and samples could be categorised
280 into two reference groups (Fig.3): agricultural diffuse source contamination only (label D+P-) or
281 agricultural diffuse and organic point source contamination (label D+P+). In the case of D+P-
282 samples, the lack of evidence for point source contamination directed by default towards diffuse
283 sources alone (artificial fertiliser and/or soil organic matter), i.e. the only N source identified in the
284 survey around the wells that could explain the high NO_3^- concentrations. In the case of D+P+ samples,
285 the impact of point source contamination was characterised, but its NO_3^- contribution relative to the
286 ubiquitous diffuse sources (whose impact was assumed) was unknown. When both steps disagreed
287 over the influence of point sources, samples were classified as D+P \pm (i.e. impact of point source
288 ambiguous).

289

290 It should be noted that this classification (and Step 2 in particular), did not discriminate between
291 septic tank and farmyard effluent contaminations, a topic of great interest in some of the literature.
292 Such differentiation would have been vain since every sampling well with a farmyard within a 300 m
293 radius also had the septic tank from the farm house within that radius.

294

295

296 **2.3.2 Statistical analysis**

297 The relationships between hydrochemical parameters and other variables (number of point sources in
298 Table SM-2) were investigated by Spearman's rank order correlation coefficients (r_s) and significance
299 levels. To compare means between categories of independent variables (% tillage, N source
300 apportionment), dependent variables (NO_3^- concentration, $\delta^{15}\text{N-NO}_3^-$ and $\delta^{18}\text{O-NO}_3^-$) were analysed in
301 the following mixed factorial model: time \times either % tillage (groups 0-50% and 50-100%) or N source
302 apportionment classification (groups D+P+, D+P- and D+P \pm as in Fig.3), with site (C, B and O) as a

303 random blocking effect. There were repeated measurements made on the experimental units (sampling
304 wells) and the correlation over time was taken into account using an unstructured covariance model.
305 Pairwise comparisons were made with Tukey-Kramer posthoc tests. The model was fitted in the
306 Mixed procedure of SAS 9.4 (2014), and all the data were log transformed because of non-constant
307 variance.

308

309

310 **3 RESULTS AND DISCUSSION**

311 **3.1 Probing NO₃⁻ source identification with groundwater quality and N source risk** 312 **assessment**

313 ***3.1.1 Introduction to groundwater quality and the NO₃⁻ contamination problem***

314 NO₃⁻ concentration in groundwater samples ranged between 2.0 and 134.9 mg L⁻¹ NO₃⁻ (median of
315 47.9 mg L⁻¹) with few low nitrate concentration samples (Fig.4). The severity of the NO₃⁻ problem in
316 the area was highlighted as 88% and 45% of the samples had NO₃⁻ concentration exceeding 25 and 50
317 mg L⁻¹, respectively. (Note that 50 mg L⁻¹ NO₃⁻ is both the EU drinking water limit for NO₃⁻ and also
318 the NO₃⁻ standard for good status of groundwater bodies under the EU Groundwater Directive). At
319 each well, NO₃⁻ concentration fluctuated between sampling events (median range of 17.5 mg L⁻¹).
320 Only four wells consistently had low NO₃⁻ concentrations (< 25 mg L⁻¹), whereas thirteen wells had
321 consistently high NO₃⁻ concentrations (> 50 mg L⁻¹).

322

323 Unlike NO₃⁻, other physico-chemical parameters complied with their respective Drinking Water
324 Directive limit, set at 200 mg L⁻¹ for Na⁺, 250 mg L⁻¹ for Cl⁻ and SO₄²⁻, between 6.0 and 9.5 for pH,
325 2500 μS cm⁻¹ for conductivity. However, these limits are elevated and may not be relevant to detect
326 pollution problems. Far more informative are the NBLs measured under uncontaminated conditions in
327 similar aquifers as defined in Tedd et al. (2017) for Irish aquifers. In that respect, parameters
328 associated with contamination from both N/non-N artificial fertiliser and animal/human waste
329 effluents (K⁺ and Cl⁻) or animal/human wastes only (Na⁺ and FC) displayed some values widely in
330 exceedance of such NBLs (Fig.4). Na⁺ varied between 4 and 46 mg L⁻¹ (median of 11), and 32% of

331 the samples exceeded the NBL reported at 13 mg L⁻¹ in Tedd et al. (2017). K⁺ varied between 0.2 and
332 63 mg L⁻¹ (median of 1.9), and 48% of the samples exceeded the NBL reported at 2.1 mg L⁻¹. As for
333 Cl⁻, it varied between 5.1 to 82.9 mg L⁻¹ (median of 29.6), and 85% of the samples exceeded the NBL
334 reported at 21 mg L⁻¹. Other parameters were equally variable: SO₄²⁻ varied between 8.8 and 68.8 mg
335 L⁻¹ (median of 31.2) and Mg²⁺ varied between 2.2 and 28.0 mg L⁻¹ (median of 14.0). From the
336 bacterial perspective, 70.2% of samples tested positive to TC, whereas 19.9% tested positive to FC.
337 Samples positive to FC originated from fifteen wells that displayed presence of FC on at least one
338 occasion. The exceedance of NBL values and the presence of FC reflect the detrimental influence of
339 anthropogenic activities (highly managed agricultural land and/or discharge of organic animal/human
340 wastes effluents from farmyards/septic tanks) on groundwater quality. Other parameters such as
341 calcium (Ca²⁺) concentration (88 to 190 mg L⁻¹, median of 122), alkalinity (210 to 526 mg CaCO₃ L⁻¹,
342 median of 308), pH (6.8 to 7.6, median of 7.3) and conductivity (584 to 1206 μS cm⁻¹, median of 784)
343 generally reflect hydrogeological conditions and limestone buffering.

344

345 In line with Fig.2, Fig.5 highlights that groundwater originated mainly from autumn and winter
346 precipitation, a period particularly conducive of NO₃⁻ leaching from agricultural soils (Premrov et al.,
347 2012). The isotopic composition of groundwater samples (δ¹⁸O-H₂O between -8.9‰ and -6.5‰, δ²H-
348 H₂O between -51.8‰ and -36.1‰), collected 170 km from the Global Network for Isotopes in
349 Precipitation (GNIP) station of Valentia Island (southwest Ireland), plotted slightly above the Local
350 meteoric Water Line (LMWL) drawn from the GNIP station data (IAEA, 2017). It was most similar
351 with winter and autumn precipitation (mean δ¹⁸O-H₂O of -6.4‰ and -6.0‰ in Fig.5, respectively). In
352 comparison, spring and summer precipitation (mean δ¹⁸O-H₂O of -4.9‰ and -4.1‰, respectively)
353 exhibited higher values. Precipitation typically displays δ²H-H₂O and δ¹⁸O-H₂O values lower in
354 winter than in summer, which is mainly controlled by the amount of water rained-out. As water
355 vapour derived from the evaporation of low-latitude oceans moves northwards with air masses, winter
356 precipitation, which is more intense than summer one because of colder condensation temperature,
357 discharges larger amounts of ²H- and ¹⁸O-enriched rainfall than during summer (Mook and de Vries,
358 2000). Consequently, remaining water vapour that reaches temperate countries like Ireland shows

359 lower $\delta^2\text{H-H}_2\text{O}$ and $\delta^{18}\text{O-H}_2\text{O}$ values in winter, which generates lower $\delta^2\text{H-H}_2\text{O}$ and $\delta^{18}\text{O-H}_2\text{O}$ values
360 in winter precipitation (in comparison with summer rainfall). In addition to the seasonal effect, $\delta^2\text{H-}$
361 H_2O and $\delta^{18}\text{O-H}_2\text{O}$ values in precipitation are also subjected to several other effects causing regional
362 and temporal variations such as the latitudinal effect (lower δ values at increasing latitude), the
363 continental effect (more negative δ values the more inland), the altitude effect (decreasing δ values at
364 higher altitude) and the amount effect (lower δ values during heavy storms) (Mook and de Vries,
365 2000).

366

367

368 ***3.1.2 Relationships between hydrochemistry and N source risk assessment: information gained*** 369 ***and limitations***

370 There were several significant yet ambiguous relationships between groundwater NO_3^- concentration
371 and chemical indicators relevant to both diffuse and point source contamination (Table 1). NO_3^-
372 concentration was positively yet weakly correlated with Na^+ concentration ($r_s = 0.133$, $p < 0.05$),
373 which could be due to the small impact of point sources (i.e. animal/human wastes effluents) on NO_3^-
374 groundwater loading. NO_3^- had a stronger positive correlation with Cl^- ($r_s = 0.342$, $p < 0.0001$), but
375 this could be indicative of contamination from diffuse applications of KCl (Section 2.1.3) and/or
376 organic point sources. No significant relationship was detected with K^+ (contained in both N-K-P
377 fertilisers and animal/human wastes), which is generally strongly held by soil particles (Weil and
378 Brady, 2017). NO_3^- was positively correlated with Ca^{2+} ($r_s = 0.479$, $p < 0.0001$), which is a major
379 component of both the widely used CAN fertiliser and subsoil/bedrock materials. NO_3^- was also
380 significantly but weakly correlated with other parameters such as SO_4^{2-} and alkalinity, whereas
381 stronger significant relationships were observed with Mg^{2+} ($r_s = -0.301$, $p < 0.0001$) and conductivity
382 ($r_s = 0.472$, $p < 0.0001$). The pH was negatively correlated with a number of parameters, but not with
383 NO_3^- , which could have otherwise been indicative of denitrification (Rivett et al., 2008). Interestingly
384 though, pH was strongly and negatively correlated with $\delta^{15}\text{N-NO}_3^-$ ($r_s = -0.513$, $p < 0.0001$) and $\delta^{18}\text{O-}$

385 NO_3^- ($r_s = -0.401$, $p < 0.0001$), which is discussed in Section 3.2.1. Many other relationships were
386 weak ($r_s < 0.3$) and/or not significant ($p > 0.05$) (Table 1).

387 Negative correlations were observed between NO_3^- concentration and the number of unsewered
388 houses ($r_s = -0.189$, $p < 0.01$) and farmyards ($r_s = -0.181$, $p < 0.01$). These relationships were
389 unexpected because a higher loading of organic waste effluents is assumed to increase NO_3^-
390 concentration. However, these correlations were also weak, which could simply indicate that point
391 sources are not major NO_3^- sources. Alternatively, the lowering of NO_3^- concentration might be due to
392 denitrification enhanced by higher DOC levels (Jahangir et al., 2014) and sustained by a higher
393 density of point sources. Nonetheless, all wells with more than ten unsewered houses within 300 m
394 radius were located in site O, where the % tillage was lower and % grassland was higher (Table SM-
395 2). Therefore, the negative correlation might be caused by land use and reduced NO_3^- leaching at site
396 O.

397

398 Other relationships in Table 1 are of particular interest. Most prominently the concentration of Na^+ ,
399 which is used as an indicator of point source contamination in Section 3.3.1, was positively correlated
400 with the number of unsewered houses ($r_s = 0.317$, $p < 0.0001$) and farmyards ($r_s = 0.247$, $p < 0.001$).
401 A closer examination of this relationship in Fig.6 reveals that in the absence of any point source
402 within a 300 m radius (i.e. no unsewered house, which also meant no farm house and its farmyard),
403 Na^+ concentration showed little variation and remained low below 9 mg L^{-1} , i.e. below the NBL of 13
404 mg L^{-1} (Tedd et al., 2017). These samples with no nearby point sources were all collected from
405 monitoring piezometers with 75-100% tillage within a 300 m radius. This ruled out high % tillage and
406 the decomposition of crop residues as an important source of Na^+ leaching. It should be noted that the
407 correlation coefficient r_s between Na^+ concentration and the number of houses further increased from
408 0.317 to 0.545 when keeping % tillage constant at 75-100%, i.e. the largest % tillage group by far
409 (65% of the samples). Added to the presence of FC in some samples (Section 3.1.1) and the fact that
410 Na^+ is a major component of organic point source effluents, these results confirm that animal/human
411 waste effluent discharges had some impact on groundwater quality. Yet these results did not inform

412 about the NO_3^- contamination source and the importance of point sources relative to the diffuse source
413 pollution.

414

415 From the landuse perspective, NO_3^- concentration was significantly higher ($p < 0.0001$) in samples
416 collected from wells with more than 50% tillage within a 300 m radius (mean of 53.3 mg L^{-1}) than if
417 % tillage was below 50% (mean of 33.7 mg L^{-1}). This is consistent with NO_3^- contamination from an
418 agricultural diffuse N sources, which could be the diffuse applications of artificial N fertiliser and/or
419 the mineralisation and nitrification of soil organic N enhanced by soil aeration post ploughing and
420 fertilisation.

421

422

423 **3.2 Investigating NO_3^- sources and dynamics using dual stable isotope analyses alone**

424 Except for two outliers slightly above 18‰, $\delta^{15}\text{N-NO}_3^-$ in groundwater ranged between 2.2‰ and
425 12.1‰ (median of 5.5‰), while $\delta^{18}\text{O-NO}_3^-$ ranged between -2.4‰ and 10.9‰ (median of 2.2‰)
426 (Fig.7). δ values in individual wells were quite stable over time. With disregard for the two outliers,
427 the temporal difference between minimum and maximum $\delta^{15}\text{N-NO}_3^-$ values was smaller than 5‰ in
428 43 wells (< 2‰ in 32 wells). Similarly, the variation in $\delta^{18}\text{O-NO}_3^-$ was below 5‰ in 42 wells (< 3‰
429 in 28 wells). Overall, both $\delta^{15}\text{N-NO}_3^-$ and $\delta^{18}\text{O-NO}_3^-$ variables were positively and significantly
430 correlated ($r_s = 0.599$, $p < 0.0001$) along a linear regression line with a slope of 0.50 (result not
431 shown).

432

433

434 **3.2.1 Biochemical and mixing processes**

435 A highly significant correlation between $\delta^{15}\text{N-NO}_3^-$ and $\delta^{18}\text{O-NO}_3^-$ ($r_s = 0.599$, $p < 0.0001$) with a
436 positive slope of 0.504 was indicative of denitrification (Granger and Wankel, 2016; Kendall et al.,
437 2007), which had been anticipated to be more limited due to the elevated levels of dissolved oxygen
438 (O_2) measured between 9 and 11 mg L^{-1} in the sand and gravel deposits of site O (Premrov et al.,
439 2012) and despite the presence of clay lenses. The strong negative correlation ($r_s = -0.513$, $p < 0.0001$)

440 between $\delta^{15}\text{N-NO}_3^-$ and groundwater pH (Table 1) may be seen as a further evidence of heterotrophic
441 denitrification as the microbial reduction of NO_3^- may induce an increase in pH (Rivett et al., 2008).

442

443 The plotting of $\delta^{15}\text{N-NO}_3^-$ against $1/\text{NO}_3^-$ concentration should in theory yield a straight line if the
444 mixing of two groundwater endmembers with distinct NO_3^- concentrations and isotopic δ values
445 occurs (Kendall et al., 2007). However no such relationship was observed (result not shown). At the
446 scale of the study area, this result provides no evidence for contamination by two N sources although
447 at a smaller scale, closer to point sources, the characteristic straight line might have been observed.
448 The characterisation of mixing processes may yet be complicated by the occurrence of denitrification
449 and the fact that the isotopic composition of end-members rarely stays constant over time (Kendall et
450 al., 2007).

451

452

453 3.2.2 NO_3^- sources

454 NO_3^- source identification based on stable isotopes is carried out by comparing $\delta^{15}\text{N-NO}_3^-$ and $\delta^{18}\text{O-}$
455 NO_3^- measured in groundwater with $\delta^{15}\text{N-NO}_3^-$ and $\delta^{18}\text{O-NO}_3^-$ expected from various N sources. The
456 expected $\delta^{15}\text{N-NO}_3^-$ values derive directly from $\delta^{15}\text{N-TN}$ (i.e. $\delta^{15}\text{N}$ in total nitrogen) measured in N
457 source materials. The mineralisation of TN into ammonium (NH_4^+) causes little isotopic fractionation
458 and $\delta^{15}\text{N-NO}_3^-$ shifts towards $\delta^{15}\text{N-TN}$ of the source as nitrification goes on in non N-limited systems
459 (Kendall et al., 2007), so N sources are expected to generate NO_3^- with $\delta^{15}\text{N-NO}_3^-$ similar to the
460 original $\delta^{15}\text{N-TN}$ values in the absence of any interfering process like denitrification. Due to its
461 atmospheric origin, $\delta^{15}\text{N-TN}$ in artificial fertilisers often varies between -4‰ and 4‰ (Wassenaar,
462 1995), which contrasts with the distinctly higher $\delta^{15}\text{N-TN}$ values in animal/human organic wastes that
463 has generally been reported to generate $\delta^{15}\text{N-NO}_3^-$ between 10‰ and 20‰ due to enhanced NH_3
464 volatilisation (Macko and Ostrom, 1994). Between these two sources, $\delta^{15}\text{N-TN}$ in soils (mostly
465 organic N) frequently varies between 4‰ and 9‰ (Heaton, 1986), although wider ranges are
466 sometimes reported (Kendall et al., 2007). In parallel to $\delta^{15}\text{N}$, $\delta^{18}\text{O-NO}_3^-$ in artificial fertilisers nitrate
467 often ranges between 18‰ and 22‰ (Amberger and Schmidt, 1987), whereas $\delta^{18}\text{O-NO}_3^-$ arising from

468 nitrification is much lower and may be expected between 0‰ and 5‰ (Durka et al., 1994), although
469 wider ranges are sometimes reported (Kendall et al., 2007). These $\delta^{15}\text{N-NO}_3^-$ and $\delta^{18}\text{O-NO}_3^-$ values
470 expected for the different types of N sources and commonly used in the literature were reported in
471 Fig.7 for comparison with δ values measured in groundwater NO_3^- . It is noteworthy that apart from
472 septic tank effluents, which had not been directly sampled in this study, artificial fertiliser commonly
473 used in the local area ($\delta^{15}\text{N-TN}$ and $\delta^{18}\text{O-NO}_3^-$), dairy slurry ($\delta^{15}\text{N-TN}$) and local agricultural soil
474 ($\delta^{15}\text{N-TN}$) samples analysed from agricultural research sites for a related soil zone study (Minet et al.,
475 2012) displayed δ values within the above-mentioned ranges.

476

477 The observed groundwater $\delta^{15}\text{N-NO}_3^-$ and $\delta^{18}\text{O-NO}_3^-$ values in Fig.7 overlapped with the expected
478 ranges from three N sources: nitrified artificial fertiliser N, soil organic N and animal/human waste N.
479 However, data interpretation should take into account the occurrence of the overall denitrification
480 line, which starts somewhere in the nitrification zone between $\delta^{15}\text{N-NO}_3^-$ of 2‰ and 6‰, i.e. between
481 the high end of the $\delta^{15}\text{N-NO}_3^-$ range expected for nitrified artificial fertiliser N and the low end of the
482 $\delta^{15}\text{N-NO}_3^-$ range expected for soil organic N-derived NO_3^- . This 2-6‰ range could be indicative of
483 the nitrification of soil organic matter that had incorporated ^{15}N -depleted nitrogen from artificial
484 fertiliser applications (Choi et al., 2017) and is later leached during groundwater recharge. This
485 interpretation of a single NO_3^- source contamination process is consistent with studies that designate
486 soil organic matter as an important source of NO_3^- leaching in intensively managed grassland (Minet
487 et al., 2012) or in tillage (Savard et al., 2010). On the other hand, the direct leaching of artificial NO_3^-
488 (contained in applied artificial fertiliser) and nitrified artificial fertiliser N (e.g. NO_3^- derived from
489 NH_4^+ in CAN) might not be an immediate source of contamination. The significantly higher NO_3^-
490 concentration where % tillage within a 300 m radius was above 50 (Section 3.1.2) was not
491 accompanied by a significant lower $\delta^{15}\text{N-NO}_3^-$ ($p > 0.05$), which could otherwise be observed with the
492 direct leaching of fertiliser-derived NO_3^- (i.e. artificial NO_3^- and nitrified fertiliser N) through the
493 unsaturated zone (Minet et al., 2012). This should not come as a surprise considering that most
494 fertiliser N applied to soil and not already taken up by plants is rapidly immobilised by soil micro-
495 organisms and therefore, little is left unused and available for leaching (Powlson et al., 1992). Had the

496 base of the denitrification line been broad enough to encompass the range of δ values expected from
497 animal/human waste point sources, more than one contamination source would have been considered
498 (Clague et al., 2015). Nevertheless, the strong positive correlations between $\delta^{15}\text{N-NO}_3^-$ and
499 concentrations of other indicators such as Na^+ ($r_s = 0.488$, $p < 0.0001$), Cl^- ($r_s = 0.363$, $p < 0.0001$) and
500 K^+ ($r_s = 0.370$, $p < 0.0001$) in Table 1 may still suggest that organic point sources play some role in
501 the contamination process, which is further discussed in Section 3.3. In comparison, there were few
502 strong and significant relationships between $\delta^{18}\text{O-NO}_3^-$ and chemical parameters.

503 The ability of soils to recycle N through MIT processes probably explains why no sample displayed
504 elevated $\delta^{18}\text{O-NO}_3^-$ values associated with artificial NO_3^- (Mengis et al., 2001). In addition, N in the
505 applied fertilisers was partly in an artificial non- NO_3^- form so that the expected $\delta^{18}\text{O-NO}_3^-$ range for
506 the entire pool of fertiliser-derived NO_3^- is lower than the 18-22‰ range for artificial NO_3^- (Minet et
507 al., 2012). Most $\delta^{18}\text{O-NO}_3^-$ values were in fact within the 0-5‰ range expected from nitrification by
508 Durka et al. (1994). This 0-5‰ range was calculated under the debatable assumption (Minet et al.,
509 2012) that the oxidation of NH_3 into nitrite (NO_2^-) incorporates without isotopic fractionation one
510 oxygen from diatomic O_2 and one oxygen from H_2O followed by the final incorporation of one
511 oxygen from H_2O during NO_2^- oxidation. If using local $\delta^{18}\text{O-H}_2\text{O}$ values (between -8.9 and -6.5‰ in
512 Fig.5) and $\delta^{18}\text{O-O}_2$ of 23.5‰ (Kroopnick and Craig, 1972), this calculated nitrification range can be
513 further narrowed to 1.9-3.5‰. It encompasses only 36% of $\delta^{18}\text{O-NO}_3^-$ values whereas a majority of
514 samples (41%) displayed values that were lower (minimum of -2.4‰). Recent research now
515 demonstrates that various kinetic isotopic fractionation factors operate during oxygen incorporations
516 and NO_2^- oxidation (Granger et al., 2016) and therefore, the calculated nitrification range of 1.9-3.5‰
517 is most likely biased. Importantly, $\delta^{18}\text{O-NO}_3^-$ of newly formed nitrate in soils or aquatic systems can
518 be deeply affected by a $\text{H}_2\text{O-NO}_2^-$ oxygen exchange and the associated equilibrium isotopic
519 fractionation (Granger and Wankel, 2016). The extent of this oxygen exchange is extremely variable
520 and it may be driven by the duration of NO_2^- accumulation, the longer the duration the larger the
521 exchange with incidentally the loss of some oxygen of diatomic O_2 origin (Buchwald et al., 2012).
522 The absence of $\delta^{18}\text{O-NO}_3^-$ values close to those of $\delta^{18}\text{O-H}_2\text{O}$ values suggests that no large oxygen
523 exchanges occurred in our study. This is consistent with the absence of NO_2^- detected in all the

524 groundwater samples (Materials and Methods SM), including those where elevated levels could have
525 been expected (contamination group D+P+ from Fig.3).

526

527

528 **3.3 Improving data interpretation by combining dual stable isotopes with indicators of point** 529 **source contamination**

530 **3.3.1 N source apportionment using indicators of point source contamination**

531 A Na⁺ CT value was calculated (based on Section 2.3.1) at 11.4 mg L⁻¹, i.e. below the 13 mg L⁻¹ NBL
532 defined in Tedd et al. (2017). As anticipated, the ‘75th percentile’ calculation excluded low NO₃⁻
533 samples with strong indications of contamination (Cl⁻ concentration between 25.6 and 63 mg L⁻¹) but
534 signs of denitrification (elevated δ¹⁵N-NO₃⁻ between 7.8 and 18.4‰). Groundwater samples could
535 then be apportioned to N source types as per the methodology in Fig.3. As a result, 22 samples
536 categorised D+P- displayed Na⁺ concentrations within a 4.0-9.0 mg L⁻¹ range (Table SM-3). They
537 were associated with contamination from agricultural diffuse N sources only (i.e. artificial fertiliser N
538 and/or soil organic matter). On the other hand, 99 samples categorised D+P+ displayed Na⁺
539 concentrations within a 11.6-46.0 mg L⁻¹ range (Table SM-3). They were associated with diffuse and
540 also point N sources (i.e. septic tanks from unsewered houses and/or farmyards). For the remaining
541 112 samples labelled D+P±, evidence of point source contamination was contradictory (‘Yes’ for
542 Step1 always followed by ‘No’ for Step2 in Fig.3) but Na⁺ concentration was within a 6.9-11.3 mg L⁻¹
543 range (Table SM-3), i.e. below the Na⁺ CT value of 11.4 mg L⁻¹. These uncertainties in group D+P±
544 possibly relate to sampling well locations (point source plumes not being intercepted), some Na⁺
545 adsorption in soil or simply low effluent discharge. Tellingly, no D+P± sample was collected from a
546 well without a nearby point source but with a Na⁺ concentration above the CT value (‘No’ for Step1
547 was never followed by ‘Yes’ for Step2 in Fig.3), which appears to confirm the validity of the two step
548 approach as this combination should not be observed. Samples collected from most wells (thirty-one
549 out of forty-four wells sampled more than once) consistently belonged to the same category, which
550 could be expected should one type of source dominate (although seasonal changes in hydrogeological
551 conditions might affect contamination processes and cause wells to switch category). It can be noted

552 that unlike Na^+ concentration, other measured parameters widely overlapped between D+P+ and D+P-
553 categories (Table SM-3), which highlights that they were probably not appropriate indicators of one
554 type of N source contamination in the context of the study area.

555
556 The contrast created by the sample classification between D+P- and D+P+ categories was useful to
557 characterise the occurrence of point source contamination in an intensively managed agricultural area.
558 However, it did not inform on the relative contributions of agricultural diffuse and organic point
559 sources to the NO_3^- issue. Although the measurement of an elevated Na^+ contamination in the vicinity
560 of septic tanks and farmyards is most likely an evidence of point source contamination, it does not
561 necessarily mean that the point source NO_3^- input to groundwater outweighs the diffuse input from
562 fertiliser- and/or soil organic matter-derived NO_3^- leached below agricultural soils. The analysis of
563 $\delta^{15}\text{N-NO}_3^-$ and $\delta^{18}\text{O-NO}_3^-$ in Section 3.3.1 aimed to resolve this uncertainty.

564

565

566 3.3.2 *Fine-tuning results interpretation*

567 The scatterplot of $\delta^{15}\text{N-NO}_3^-$ and $\delta^{18}\text{O-NO}_3^-$ superimposed on the N source apportionment
568 classification for groundwater samples is presented in Fig.7. The effect of classification on $\delta^{15}\text{N-NO}_3^-$
569 was significant ($p < 0.0001$), with all pairwise comparisons between groups also significant. D+P-
570 values (mean $\delta^{15}\text{N-NO}_3^-$ of 4.4‰) were significantly lower ($p < 0.0001$) than D+P+ values (mean
571 $\delta^{15}\text{N-NO}_3^-$ of 7.1‰). D+P± values were intermediate (mean $\delta^{15}\text{N-NO}_3^-$ of 5.2‰), significantly higher
572 than D+P- values ($p = 0.005$) and significantly lower than D+P+ values ($p < 0.0001$). The reason for
573 these differences between groups may relate to the differential occurrence of denitrification, as
574 significant positive relationships between $\delta^{15}\text{N-NO}_3^-$ and $\delta^{18}\text{O-NO}_3^-$ were detected in groups D+P+ (r_s
575 = 0.650, $p < 0.0001$) and D+P± ($r_s = 0.618$, $p < 0.0001$), but not in group D+P- (Fig.7). The fact that
576 $\delta^{15}\text{N-NO}_3^-$ values in group D+P+ were higher than in group D+P± suggests a more advanced
577 denitrification (i.e. less NO_3^- left in groundwater) where point source contamination was clearly
578 characterised. In comparison with $\delta^{15}\text{N-NO}_3^-$, no significant classification effect ($p > 0.05$) was
579 detected for $\delta^{18}\text{O-NO}_3^-$, possibly because $\delta^{18}\text{O-NO}_3^-$ is less affected by denitrification than $\delta^{15}\text{N-NO}_3^-$.

580

581 The denitrification lines for the D+P+ and D+P± groups started in the same $\delta^{15}\text{N-NO}_3^-$ zone of 2-6‰
582 (Fig.7) as all but one D+P- sample (sample with $\delta^{15}\text{N-NO}_3^-$ of 18.6‰), a range that could be related to
583 nitrification from soil organic matter that has incorporated ^{15}N -depleted nitrogen from artificial
584 fertilisers (Section 3.2.2). This interpretation with well defined denitrification lines that have the same
585 origin ruled out the discharge of animal/human waste effluents from point sources as a main
586 contributor to groundwater NO_3^- contamination, which should have otherwise broaden the distribution
587 of $\delta^{15}\text{N-NO}_3^-$ towards higher values making the characterisation of denitrification possibly more
588 difficult (Clague et al., 2015). Instead, we hypothesise that point source discharge increased the levels
589 of DOC in the vicinity of wells, which promoted reducing conditions for NO_3^- and therefore
590 denitrification observed with most samples (groups D+P+ and D+P ± represented 211/233 samples,
591 and 40/45 sampling wells). The seemingly lesser denitrification affecting D+P± samples may just
592 reflect a more limited impact of point sources at these sampling wells. The absence of a positive
593 relationship observed between $\delta^{15}\text{N-NO}_3^-$ and $\delta^{18}\text{O-NO}_3^-$ with samples D+P- confirmed the original
594 hypothesis that despite the presence of clay lenses, the free-draining nature of the subsoil combined
595 with the high O_2 level and low DOC (Premrov et al., 2012) limited the potential for denitrification.
596 The examination of Fig.7 and group D+P- in particular also suggests that some synthetic fertiliser
597 NO_3^- may have leached down to groundwater as some D+P- samples with low $\delta^{15}\text{N-NO}_3^-$ value (3.4-
598 3.9‰) exhibited $\delta^{18}\text{O-NO}_3^-$ distinctly higher (6.6-8.0‰). However, this was unusual and the direct
599 leaching of artificial fertiliser NO_3^- was not widespread in the study area, despite conditions that might
600 have favoured it (shallow water-table overlain by free-draining soil, elevated precipitation, high
601 fertiliser application rates). Similar results, also observed in the unsaturated zone (Minet et al., 2012),
602 were not surprising since soil microbes usually leave very little nitrate unused in soil following
603 application (Section 3.2.2).

604

605 In the context of the study area, dual stable isotopes used alone (Section 3.2.2) helped identify the
606 most likely main contributor to groundwater NO_3^- contamination (nitrification of soil organic matter
607 as an agricultural diffuse source, which is stimulated by fertiliser application and tillage) as well as

608 characterise denitrification. The combined use of two contamination indicators (as described in Fig.3)
609 with δ values helped identify conditions for denitrification to take place, i.e. the presence of organic
610 point sources near sampling wells. In a more complex environment, this methodology and the use of
611 additional indicators of contamination, e.g. pharmaceutical molecules specific to animals or to
612 humans (Fenech et al., 2012) added to Fig.3 classification, could help further categorise groundwater
613 samples and differentiate between NO_3^- contamination from septic tanks and from farmyard sources,
614 which could not be achieved with Na^+ concentration.

615

616

617 4 CONCLUSIONS

- 618 ▪ Plotting $\delta^{15}\text{N}-\text{NO}_3^-$ against $\delta^{18}\text{O}-\text{NO}_3^-$ revealed a strong significant correlation between both
619 variables ($p < 0.0001$, $r_s = 0.599$, slope of 0.5), which was indicative of denitrification. After
620 comparison with the δ values expected from various N sources, the origin of the regression line
621 suggested that groundwater contamination by NO_3^- was dominated by an agricultural diffuse N
622 source (most likely the large organic matter pool that has incorporated ^{15}N -depleted nitrogen from
623 artificial fertiliser in agricultural soils).
- 624 ▪ Two indicators of organic point source contamination, presence/absence of organic point sources
625 (i.e. septic tank and/or farmyard) near sampling wells and exceedance/non-exceedance of a
626 contamination threshold value for Na^+ in groundwater, showed their relevance to characterise the
627 influence of organic point sources on groundwater quality in many groundwater samples.
- 628 ▪ The classification of groundwater samples according to the combination of both indicators
629 followed by the analysis of the scatterplot of $\delta^{15}\text{N}-\text{NO}_3^-$ against $\delta^{18}\text{O}-\text{NO}_3^-$ showed that
630 denitrification occurred only in samples where point source contamination was characterised or
631 suspected, possibly because of a high DOC concentration in groundwater.
- 632 ▪ Combining contamination indicators and a large stable isotopes dataset collected over a large study
633 area helped i) to identify the main source of groundwater NO_3^- and ii) to associate the
634 occurrence/non-occurrence of a microbial process (denitrification) to one type of contamination

635 (organic point source), which improved our understanding of NO₃⁻ contamination processes in
636 groundwater.

637

638

639 **ACKNOWLEDGEMENTS**

640 The authors thank Enterprise Ireland for funding this project through their Basic Research Grants
641 Scheme. We are grateful to staff from Trinity College Dublin and Queen's University Belfast for their
642 support during chemical and isotope analyses, to Jim Grant (Statistics and Applied Physics, Teagasc)
643 for providing statistical analysis, to Simon Leach (Agricultural Catchment Programme, Teagasc) for
644 creating maps and to three anonymous reviewers for their constructive comments. The authors wish to
645 thank Teagasc from Oak Park Research Centre for permitting piezometer installation and groundwater
646 sampling, and all the landowners from the Barrow Valley study area who kindly gave access to their
647 water supplies.

648

649

650 **REFERENCES**

651 Amberger, A., Schmidt, H.L., 1987. Natürliche Isotopengehalte von Nitrat als Indikatoren für dessen
652 Herkunft. *Geochemica et Cosmochemica Acta* 51, 2699-2705.

653 Buchwald, C., Santoro, A.E., McIlvin, .R., Casciotti, K.L., 2012. Oxygen isotopic composition of
654 nitrate and nitrite produced by nitrifying cocultures and natural marine assemblages. *Limnology*
655 *and Oceanography* 57, 1361-1375

656 Choi, W.-J., Kwak, J.-H., Lim, S.-S., Park, H.-J., Chang, S.X., Lee, S.-M., Arshad, M.A., Yun, S.-I.,
657 Kim, H.-Y., 2017. Synthetic fertilizer and livestock manure differently affect $\delta^{15}\text{N}$ in the
658 agricultural landscape: a review. *Agriculture, Ecosystems and Environment* 237, 1-15.

659 Clague, J.C., Stenger, R., Clough, T.J., 2015. Evaluation of the stable isotope signatures of nitrate to
660 detect denitrification in a shallow groundwater system in New Zealand. *Agriculture, Ecosystems*
661 *and Environment* 202, 188-197.

662 Coxon, C.E., Thorn, R.H., 1991. Nitrates, groundwater and the Nitrate Directive. In: Feehan, J. (Ed.)
663 Environment and development in Ireland. Environmental Institute, University College Dublin,
664 Dublin, Ireland, pp. 483-486.

665 Daly E.P., 1981. Nitrate levels in the aquifers of the Barrow River Valley. Geological Survey of
666 Ireland Report, May 1981, Dublin, Ireland.

667 Davis, P., Syme, J., Heikoop, J., Fessenden-Rahn, J., Perkins, G., Newman, B., Chrystal, A.E.,
668 Hagerty, S.B., 2015. Quantifying uncertainty in stable isotope mixing models. *Journal of*
669 *Geophysical Research: Biogeosciences* 120, 903–923

670 Durka, W., Schulze, E.D., Gebauer, G., Voerkelius, S., 1994. Effects of forest decline on uptake and
671 leaching of deposited nitrate determined from ^{15}N and ^{18}O measurements. *Nature* 372, 765-767.

672 EPA (Environmental Protection Agency), 2017. EPA Map Viewer, interactive Land map (Corine
673 Land Cover 2000). Accessible at: <http://gis.epa.ie/Envision> (accessed 20/02/2017).

674 Fenech, C., Rock, L., Nolan, K., Tobin, J., Morrissey, A., 2012. The potential for a suite of isotope
675 and chemical markers to differentiate sources of nitrate contamination: a review. *Water Research*
676 46, 2023-2041.

677 Fogg, G.E., Rolston, D.E., Decker, D.L., Louie, D.T., Grismer, M.E., 1998. Spatial variation in
678 nitrogen isotope value beneath nitrate contamination sources. *Ground Water* 36, 418-426.

679 Granger, J., Wankel, S.D., 2016. Isotopic overprinting of nitrification on denitrification as a
680 ubiquitous and unifying feature of environmental nitrogen cycling. *Proceedings of the National*
681 *Academy of Sciences of the United States of America* 113, E6391-E6400.

682 GSI (Geological Survey of Ireland), 2017. Groundwater Data Viewer, interactive maps. Accessible at:
683 <http://spatial.dcenr.gov.ie/GeologicalSurvey/Groundwater/index.html> (accessed 20/02/2017).

684 Heaton, T.H.E., 1986. Isotopic studies of nitrogen pollution in the hydrosphere and atmosphere: a
685 review. *Chemical Geology (Isotope Geoscience Section)* 59, 87-102.

686 Hosono, T., Tokunaga, T., Kagabu, M., Nakata, H., Orishikida, T., Lin, I.-T., Shimada, J., 2013. The
687 use of $\delta^{15}\text{N}$ and $\delta^{18}\text{O}$ tracers with an understanding of groundwater flow dynamics for evaluating
688 the origins and attenuation mechanisms of nitrate pollution. *Water Research* 47, 2661-2675

689 Hughes, C.E., Crawford, J., 2012. A new precipitation weighted method for determining the meteoric
690 water line for hydrological applications demonstrated using Australian and global GNIP data.
691 Journal of Hydrology 464-465, 344-351.

692 IAEA (International Atomic Energy Agency), 2017. Global Network of Isotopes in Precipitation. The
693 GNIP Database. Accessible at: <http://www.iaea.org/water> (accessed 20/02/2017).

694 Jahangir, M.M.R., Minet, E.P., Johnston, P., Premrov, A., Coxon, C.E., Hackett, R., Richards, K.G.,
695 2014. Mustard catch crop enhances denitrification in shallow groundwater beneath a spring
696 barley field. Chemosphere 103, 234-239.

697 Kendall, C., Elliott, E.M., Wankel, S.D., 2007. Tracing anthropogenic inputs of nitrogen to
698 ecosystems. In: Michener, R.H., Lajtha, K. (Ed.), Stable Isotopes in Ecology and Environmental
699 Science. Blackwell Publishing, Oxford, pp. 375-449.

700 Kim, K.-H., Yun, S.-T., Mayer, B., Lee, J.-H., Kim, T.-S., Kim, H.-K., 2015. Quantification of nitrate
701 sources in groundwater using hydrochemical and dual isotopic data combined with a Bayesian
702 mixing model. Agriculture, Ecosystems and Environment 199, 369-381.

703 Macko, S.A., Ostrom, N.E., 1994. Molecular and pollution studies using stable isotopes. In: Lajtha,
704 K., Michner, R.M. (Ed.) Stable Isotopes in Ecology and Environmental Sciences. Blackwell
705 Scientific Publishers, Oxford, pp. 45-62.

706 Mengis, M., Walther, U., Bernasconi, S.M., Wehrli, B., 2001. Limitations of using $\delta^{18}\text{O}$ for the source
707 identification of nitrate in agricultural soils. Environmental Science and Technology 35, 1840-
708 1844.

709 Minet, E., Goodhue, R., Coxon, C.E., Kalin, R.M., Meier-Augenstein, W., 2011. Simplifying and
710 improving the extraction of nitrate from freshwater for stable isotope analyses. Journal of
711 Environmental Monitoring 13, 2062-2066.

712 Minet, E., Coxon, C.E., Goodhue, R., Richards, K.G., Kalin, R.M., Meier-Augenstein, W., 2012.
713 Evaluating the utility of ^{15}N and ^{18}O isotope abundance analyses to identify nitrate sources: a soil
714 zone study. Water Research 46, 3723-3736.

715 Mook, W.G., de Vries, J.J., 2000. Environmental Isotopes in the Hydrological Cycle: Principles and
716 Applications, vol. 1: Theory, Methods, Review. Accessible at: [http://www-](http://www-naweb.iaea.org/napc/ih/IHS_resources_publication_hydroCycle_en.html)
717 [naweb.iaea.org/napc/ih/IHS_resources_publication_hydroCycle_en.html](http://www-naweb.iaea.org/napc/ih/IHS_resources_publication_hydroCycle_en.html) (accessed 10/07/2017).

718 Mulqueen, J., Rodgers, M., Bouchier, H., 1999. Land application of organic manures and silage
719 effluent - project report 4025. Teagasc, Dublin, Ireland.

720 Oenema, O., Bleeker, A., Braathen, N.A., Budňáková, M., Bull, K., Čermák, P., Geupel, M., Hicks,
721 K., Hoft, R., Kozlova, N., Leip, A., Spranger, T., Valli, L., Velthof, G., Winiwarter, W., 2011.
722 Nitrogen in current European policies. In: Sutton, M.A., Howard, C.M., Erisman, J.W., Billen, G.,
723 Bleeker, A., Grennfelt, P., van Grinsven, H., Grizzetti, B. (Ed.) The European Nitrogen
724 Assessment. Cambridge University Press, pp. 62-81.

725 Pastén-Zapata, E., Ledesma-Ruiz, R., Harter, T., Ramírez, A.I., Mahlkecht, J., 2014. Assessment of
726 sources and fate of nitrate in shallow groundwater of an agricultural area by using a multi-tracer
727 approach. *Science of the Total Environment* 470-471, 855-864.

728 Powlson, D.S., Hart, P.B.S., Poulton, P.R., Johnston, A.E., Jenkinson, D.S., 1992. Influence of soil
729 type, crop management and weather on the recovery of ¹⁵N-labelled fertilizer applied to winter
730 wheat in spring. *Journal of Agricultural Science* 118, 83-100.

731 Premrov, A., Coxon, C.E., Hackett, R., Kirwan, L., Richards, K.G., 2012. Effects of over-winter
732 green cover on groundwater nitrate and dissolved organic carbon concentrations beneath tillage
733 land. *Science of the Total Environment* 438, 144-153.

734 Ranjbar, F., Jalali, M., 2012. Calcium, magnesium, sodium and potassium release during
735 decomposition of some organic residues. *Communications in Soil Science and Plant Analysis* 43,
736 645-659.

737 Richards, S., Paterson, E., Withers, P.J.A., Stutter, M., 2016. Septic tank discharges as multi-pollutant
738 hotspots in catchments. *Science of the Total Environment* 542, 854-863.

739 Rivett, M.O., Buss, S.R., Morgan, P., Smith, J.W.N., Bemment, C.D., 2008. Nitrate attenuation in
740 groundwater: A review of biogeochemical controlling processes. *Water Research* 42, 4215-4232.

741 Robertson, W.D., Cherry, J.A., Sudicky, E.A., 1991. Ground-water contamination from two small
742 septic systems on sand aquifers. *Ground Water* 29, 82-92.

743 SAS, 2014. SAS/STAT1 9.4 User's Guide. SAS Institute Inc., Cary, NC.

744 Savard, M.M, Somers, G., Smirnoff, A., Paradis, D., van Bochove, E., Liao, S., 2010. Nitrate isotopes
745 unveil distinct seasonal N-sources and the critical role of crop residues in groundwater
746 contamination. *Journal of Hydrology* 381, 134-141.

747 Sommer, S.G., Husted, S., 1995. The chemical buffer system in raw and digested animal slurry.
748 *Journal of Agricultural Science* 124, 45-53.

749 Stark, C.H., Richards, K.G., 2008. The continuing challenge of nitrogen loss to the environment:
750 environmental consequences and mitigation strategies. *Dynamic Soil, Dynamic Plant* 2, 41-55.

751 Stoewer, M.M., Knöller, K., Stumpp, C., 2015. Tracing freshwater nitrate sources in pre-alpine
752 groundwater catchments using environmental tracers. *Journal of Hydrology* 524, 753-767.

753 Sutton, M.A., Oenema, O., Erisman, J.W., Leip, A., van Grinsven, H., Winiwarer, W., 2011. Too
754 much of a good thing. *Nature* 472, 159-61.

755 Tedd, K., Coxon, C.E., Misstear, B., Daly, D., Craig, M., Mannix, A., Hunter Williams, T., 2017.
756 Assessing and developing Natural Background Levels for chemical parameters in Irish
757 groundwater. EPA Research Report 2007-FS-WQ-16-S4. Environmental Protection Agency,
758 Wexford, Ireland.

759 van Grinsven, H.J.M., ten Berge, H.F.M., Dalgaard, T., Fraters, B., Durand, P., Hart, A., Hofman, G.,
760 Jacobsen, B.H., Lalor, S.T.J., Lesschen, J.P., Osterburg, B., Richards, K.G., Techen, A.-K.,
761 Vertès, F., Webb, J., Willems, W.J., 2012. Management, regulation and environmental impacts
762 of nitrogen fertilization in northwestern Europe under the Nitrates Directive; a benchmark study.
763 *Biogeosciences* 9, 5143-5160.

764 Wassenaar, L.I., 1995. Evaluation of the origin and fate of nitrate in Abbotsford aquifer using the
765 isotopes of ^{15}N and ^{18}O in NO_3^- . *Applied Geochemistry* 10, 391-405.

766 Weil, R.R., Brady, N.C., 2017. The colloidal fraction: seat of soil chemical and physical activity. In:
767 Fox, D., Gilfillan, A. (Ed.) *The Nature and Properties of Soils*, 15th Edition, Chapter 8. Pearson
768 Education, Inc.

769 Wells, N.S., Hakoun, V., Brouyère, S., Knöller, K., 2016. Multi-species measurements of nitrogen
770 isotopic composition reveal the spatial constraints and biological drivers of ammonium
771 attenuation across a highly contaminated groundwater system. *Water Research* 98, 363-375.
772 Xue, D., Botte, J., De Baets, B., Accoe, F., Nestler, A., Taylor, P., Van Cleemput, O., Berglund, M.,
773 Boeckx, P., 2009. Present limitations and future prospects of stable isotope methods for nitrate
774 source identification in surface- and groundwater. *Water Research* 43, 1159-1170.
775 Xue, D., Pang, F., Meng, F., Wang, Z., Wu, W., 2015. Decision-tree-model identification of nitrate
776 pollution activities in groundwater: a combination of a dual isotope approach and chemical ions.
777 *Journal of Contaminant Hydrology* 180, 25-33.

778

779

780 LIST OF FIGURES

781 Figure 1: Study area with sampling well locations (n = 45), 10 m elevation contour lines (m above sea
782 level), gravel and bedrock aquifer boundaries (adapted from GSI (2017), with ‘Extended gravel’
783 area referring to fluvio-glacial sand and gravel with thickness ≥ 9 m at wells C5 and C10 and
784 therefore suggested as part of the gravel aquifer).

785 Figure 2: Daily effective rainfall (mm), soil moisture deficit or SMD (mm), mean daily air
786 temperature ($^{\circ}\text{C}$) and mean groundwater temperature (mean for each sampling campaign \pm
787 standard deviation). (Shaded boxes on the time axis refer to the different sampling campaigns.)

788 Figure 3: Framework to classify groundwater samples and apportion contamination to the following
789 types of N sources: D+P+ (Diffuse and Point), D+P- (Diffuse only) and D+P \pm (Diffuse, Point
790 ambiguous). (CT stands for Na^+ contamination threshold, as defined in Section 2.3.1.; averages
791 and ranges of values for each measured physico-chemical parameter within each contamination
792 group are presented in Table SM-3.)

793 Figure 4: Boxplots of ion concentrations (NO_3^- , Na^+ , K^+ , Cl^- , SO_4^{2-} , Mg^{2+} and Ca^{2+} in mg L^{-1}), pH (pH
794 units), alkalinity ($\text{mg CaCO}_3 \text{ L}^{-1}$) and conductivity ($\mu\text{S cm}^{-1}$). (Boxes represent the central half of
795 the data, with the bar in the middle as the median; start of left whisker and end of the right

796 whisker represents the lowest and highest values that are not outliers; circles are outliers outside
797 10th and 90th percentiles.)

798 Figure 5: Scatterplot of $\delta^{18}\text{O}\text{-H}_2\text{O}$ and $\delta^2\text{H}\text{-H}_2\text{O}$ (‰ VSMOW) in groundwater samples collected in
799 the Barrow Valley study area between September 2002 and 2003 (n = 118) and precipitation
800 collected at the Irish GNIP station of Valentia Island between January 2000 and September 2003
801 (n = 45) (astronomical seasons based on spring and autumnal equinoxes, winter and summer
802 solstices). (The solid Ordinary Least Square regression line (Hughes and Crawford, 2012), with
803 Spearman Rank correlation coefficient and p value, represents the meteoric water line for
804 Valentia Island precipitation.)

805 Figure 6: Scatterplot of Na^+ concentration and the number of unsewered houses within a 300 m radius
806 (samples from well B6 and C10 excluded because of communal septic tanks, n = 222).

807 Figure 7: Scatterplot of $\delta^{15}\text{N}\text{-NO}_3^-$ (‰ Air) and $\delta^{18}\text{O}\text{-NO}_3^-$ (‰ VSMOW) in groundwater samples
808 across the following categories of N source contamination: D+P+ (Diffuse and Point, n = 99),
809 D+P- (Diffuse only, n = 22) and D+P± (Diffuse but point uncertain, n = 112). (Regression lines
810 apply only to D+P+ and D+P± groups where relationships were significant; arrows describing
811 microbial processes and boxes that delineate commonly expected δ values for NO_3^- derived from
812 several N sources present in the study area are reported in the following references: Wassenaar
813 (1995) for artificial fertiliser $\delta^{15}\text{N}$, Heaton (1986) for soil $\delta^{15}\text{N}$, Macko and Ostrom (1994) for
814 animal/human waste $\delta^{15}\text{N}$, Amberger and Schmidt (1987) for artificial fertiliser $\delta^{18}\text{O}$, Durka et al.
815 (1994) for nitrification $\delta^{18}\text{O}$, Mengis et al. (2001) for MIT processes, Granger and Wankel (2016)
816 for denitrification.)

817

818

819 LIST OF TABLES

820 Table 1: Correlation matrix of Spearman's rank correlation coefficients r_s between hydrochemical and
821 stable isotopes (in NO_3^-) variables and the number of point sources (unsewered houses,
822 farmyards) within 300 m radius around sampling wells. (Significance levels: $p \leq 0.05$ *, $p \leq 0.01$

823 **, $p \leq 0.001$ ***, $p \leq 0.0001$ ****; correlations with $p > 0.05$ not reported; relationships with r_s
824 > 0.3 are shaded.)

825

826

827 **LIST OF SUPPLEMENTARY MATERIALS**

828 Figure SM-1: Land use in the Barrow Valley sampling area in 2000, with boundaries of the Electoral
829 Divisions (adapted from EPA (2017)).

830 Table SM-1: Description of the sampling wells (ND stands for Not Determined).

831 Table SM-2: Point N sources (farmyards, houses) and diffuse N sources (includes % agricultural land
832 and % tillage) present within 300 m radius of sampling wells.

833 Table SM-3: Averages and ranges of measured physico-chemical parameters within the following
834 contamination groups: D+P+ (Diffuse and Point, $n = 99$), D+P- (Diffuse only, $n = 22$) and D+P±
835 (Diffuse but point uncertain, $n = 112$).

836 Materials and Methods SM

Table 1[Click here to download Table: Table 1_revised.docx](#)**Table 1**

Table 1: Correlation matrix of Spearman's rank correlation coefficients r_s between hydrochemical and stable isotopes (in NO_3^-) variables and the number of point sources (unsewered houses, farmyards) within 300 m radius around sampling wells. (Significance levels: $p \leq 0.05$ *, $p \leq 0.01$ **, $p \leq 0.001$ ***, $p \leq 0.0001$ ****; correlations with $p > 0.05$ not reported; strongest relationships with $r_s > 0.3$ are shaded.)

Parameter	NO_3^-	Cl^-	K^+	Na^+	SO_4^{2-}	Mg^{2+}	Ca^{2+}	pH	Conductivity	Alkalinity	$\delta^{15}\text{N-NO}_3^-$	$\delta^{18}\text{O-NO}_3^-$
Cl⁻	0.342****											
K⁺	-	0.251***										
Na⁺	0.133*	0.715****	0.366****									
SO₄²⁻	0.256****	0.191**	0.180**	0.259****								
Mg²⁺	-0.301****	-	-0.168*	-								
Ca²⁺	0.479****	0.293****	0.304****	0.256****	0.242***	-0.331****						
pH	-	-0.203**	-0.359****	-0.252**	-	-	-0.417****					
Conductivity	0.472****	0.581****	0.413****	0.539****	0.442****	-	0.787****	-0.504****				
Alkalinity	-0.179**	-	0.386****	0.139*	-	0.183**	0.347****	-0.629****	0.471****			
$\delta^{15}\text{N-NO}_3^-$	-	0.363****	0.370****	0.488****	0.335****	-	0.321****	-0.513****	0.544****	0.493****		
$\delta^{18}\text{O-NO}_3^-$	-0.281****	-	-	0.159*	0.141*	-	-	-0.401****	0.231***	0.453****	0.599****	
Houses^a	-0.189**	0.146*	-	0.317****	-	0.192**	-	-	-	-	0.168*	-
Farmyards	-0.181**	0.298****	-	0.247***	-	0.331****	-	-	0.225**	0.182**	0.457****	0.226**

Figure 1

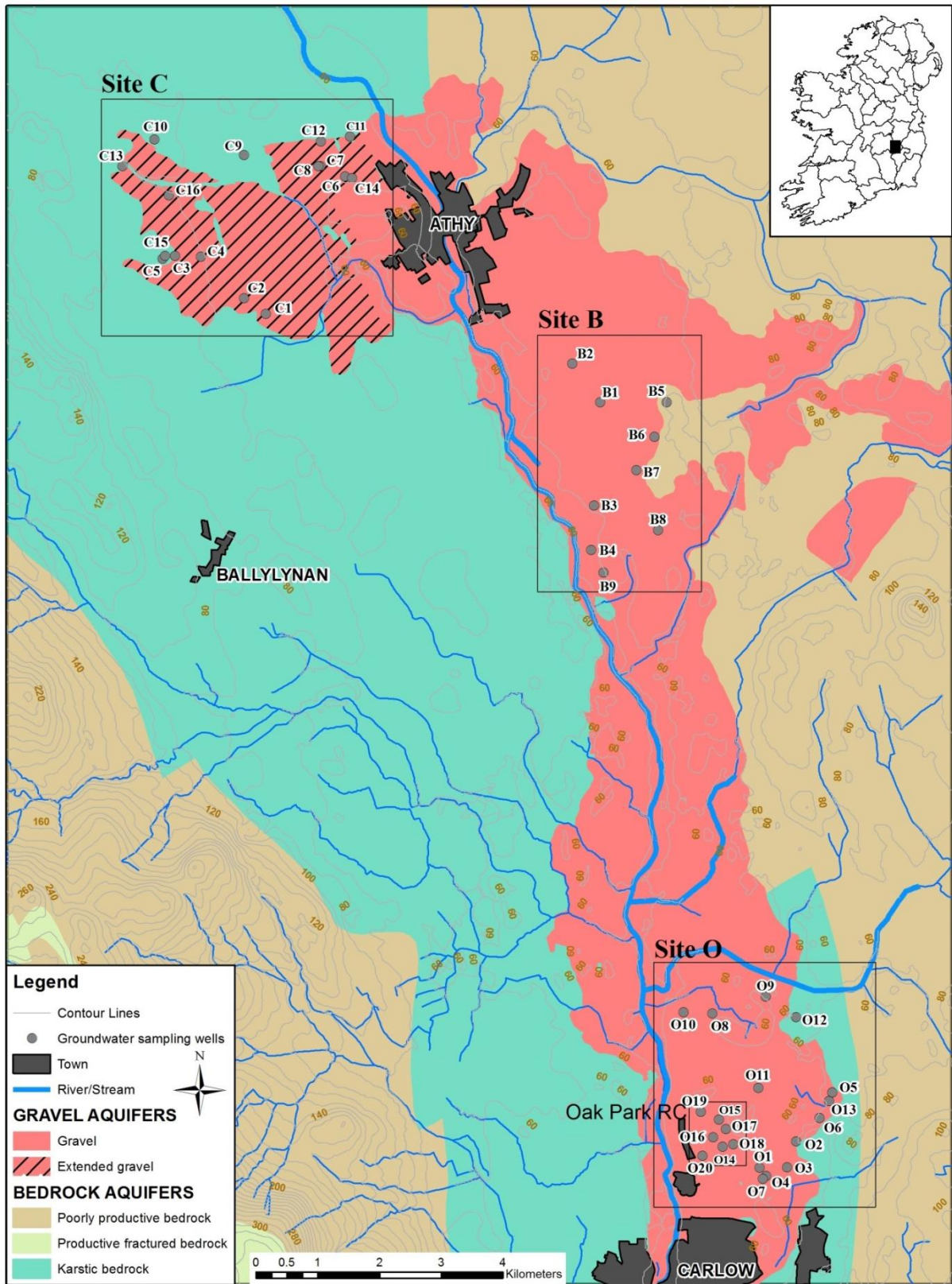


Figure 2

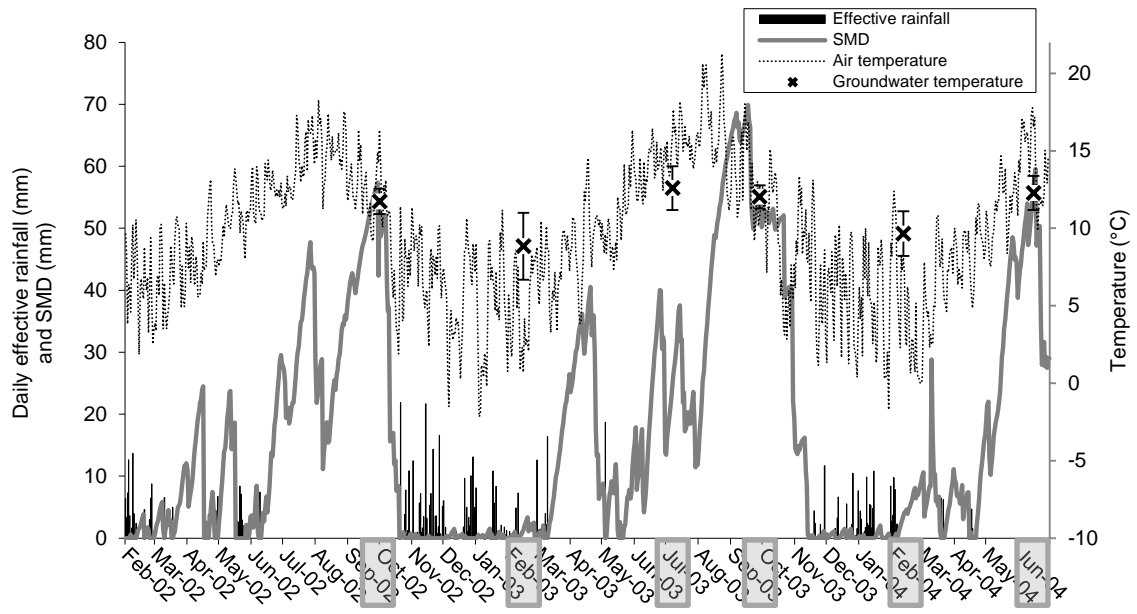


Figure 3

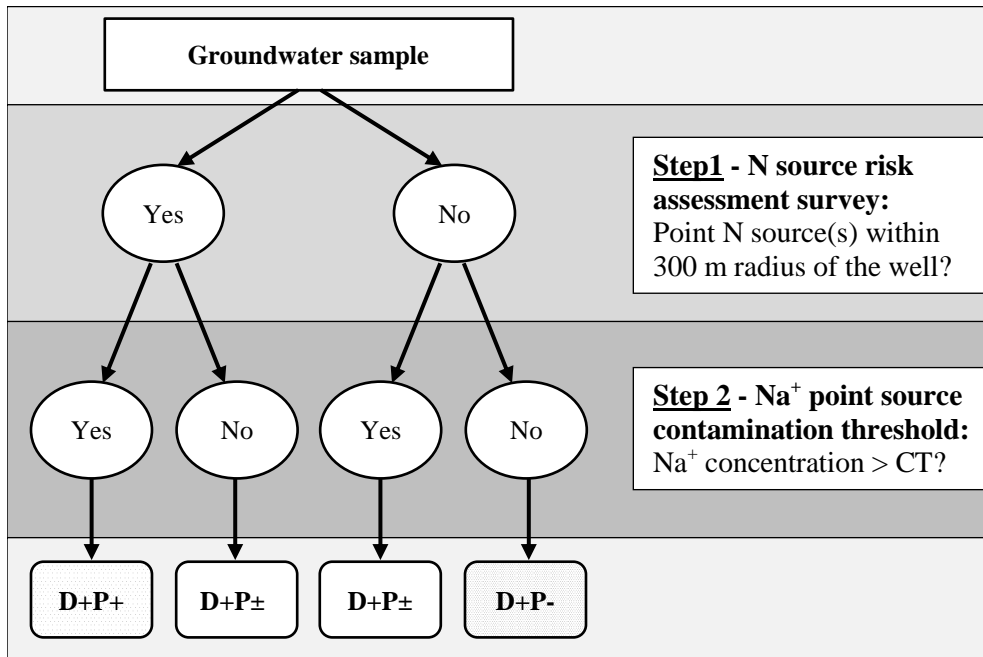


Figure 4

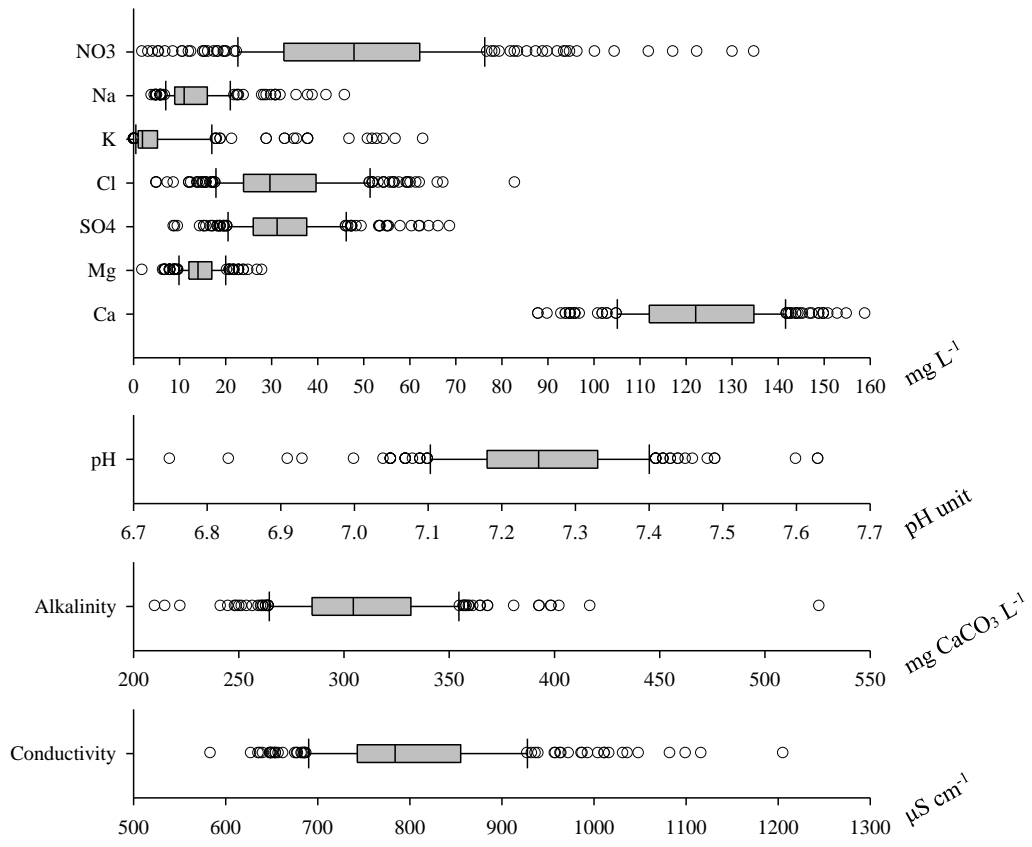


Figure 5

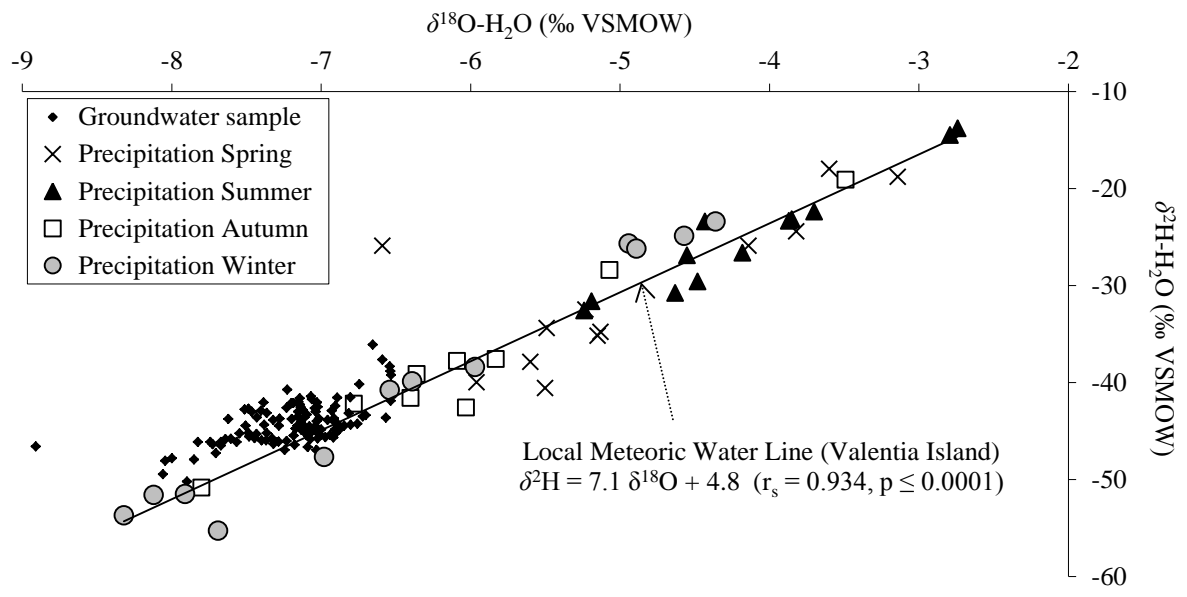


Figure 6

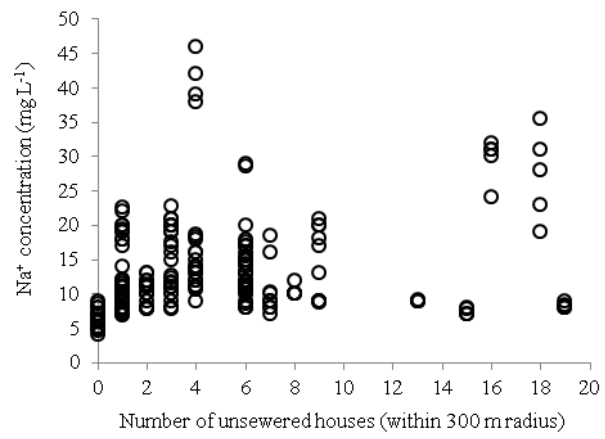


Figure 7

